Deep learning solution method for heterogeneous firm models

Yoshiya Yokomoto, Keio University

April 2, 2025

Abstract

Abstract

This paper introduces a novel solution method for heterogeneous firm models with aggregate uncertainty that significantly reduces computational time while maintaining solution accuracy. The core innovation involves approximating the policy function with a neural network that includes the equilibrium price as a state variable. This strategy directly tackles the fundamental computational bottleneck of repeated market-clearing equilibrium price calculations during simulation, leveraging the neural network's ability to handle the resulting high-dimensional state space and overcome the curse of dimensionality. Applied to seminal models in the literature, including Khan and Thomas (2008) and Bloom et al. (2018), this approach achieves speed improvements of up to 50x. By maintaining the skeleton of established solution techniques while replacing key components with neural network approximations, my approach remains transparent and accessible to researchers already familiar with standard heterogeneous agent modeling techniques, opening new possibilities for analyzing complex firm dynamics with realistic computational resources.

1 Introduction

This paper introduces a novel global solution method that delivers dramatic computational speed improvements for solving heterogeneous firm models with aggregate uncertainty. By combining deep learning neural networks with traditional solution techniques, I address the curse of dimensionality that has been a persistent challenge in these models. My approach maintains the established distribution-tracking methods used in the literature while substantially accelerating the process of finding equilibrium prices in each simulation period. Applied to seminal heterogeneous firm models like Bloom et al. (2018), my method achieves speed improvements of up to 50x while maintaining solution accuracy. My main contributions are threefold:

First, I provide global solutions that capture potential non-linearities in general equilibrium models with stochastic business cycle simulations. Unlike approximation methods that may miss critical non-linear relationships, my approach preserves the rich dynamics of heterogeneous firm models while making them computationally tractable.

Second, my method delivers solutions that are orders of magnitude faster while maintaining the accuracy achieved by existing solution methods. This speed advantage proves particularly valuable when working with heterogeneous firm frameworks that previously required prohibitive computation times. For example, in applications to models such as Bloom et al. (2018), my approach reduces computation time from approximately 40 hours to around 50 minutes while preserving—and in some cases improving—solution accuracy. This efficiency gain is especially important for models with rich firm heterogeneity and aggregate uncertainty, where computational demands have historically limited their practical application.

Third, I preserve the skeleton of existing solution methods that are well-recognized and well-understood in the literature, particularly as surveyed in Terry (2017). By maintaining structural similarity to established techniques like the Krusell-Smith algorithm, my approach remains accessible to researchers already familiar with these methods. I replace key components of traditional methods with neural network approximations while keeping the overall solution structure intact, making my innovations immediately applicable to a wide range of heterogeneous firm models.

I achieve these improvements through state-of-the-art deep learning techniques utilizing neural networks. My approach overcomes the curse of dimensionality in models with large state spaces, which is particularly acute in heterogeneous firm models where both the distribution of firm-specific states and aggregate variables must be tracked simultaneously. Neural networks excel at handling these high-dimensional problems, allowing my method to efficiently navigate the expansive state spaces characteristic of heterogeneous firm models like Khan and Thomas (2008) and Bloom et al. (2018). Additionally, I leverage GPU acceleration to dramatically enhance computational performance for models with millions of potential state-space combinations.

The specific novelty of my approach lies in substantially speeding up the stochastic simulation process where finding equilibrium prices in each simulation period is required. In heterogeneous firm models with aggregate uncertainty, market-clearing conditions must be satisfied in each period, requiring iterations to find equilibrium prices that balance aggregate supply and demand. Traditional methods iterate repeatedly to find these market-clearing prices at each point in the simulation, creating a significant computational bottleneck. My neural network approach learns optimal responses across the state space, eliminating the need for costly repetitive optimization within the simulation loop. This particular computational challenge has been a persistent obstacle for researchers working with heterogeneous firm models, and my method specifically targets this well-defined problem, providing a solution that maintains accuracy while delivering significant performance improvements.

To demonstrate the method's practicality and robustness, this paper applies our approach to two prominent heterogeneous firm models. First, it is applied to Khan and Thomas (2008), which features firm heterogeneity in terms of capital levels and idiosyncratic productivity shocks. Second, the methodology is extended to a more complex setting presented byBloom et al. (2018), where firms are subjected to stochastic volatility shocks alongside two endogenous state variables, resulting in over three million state-space combinations. Our results show that the neural network approach not only matches the key macroeconomic dynamics, microeconomic moments, and forecasting accuracy reported in these papers but does so with substantially reduced computational requirements.

The rest of the paper is organized as follows. In the next section, I will survey the related literature. Section 2 introduces our methodology in the context of the Khan and Thomas (2008) model, contrasting our neural network approach with the traditional Krusell-Smith solution technique, and presents comprehensive results comparing the performance, accuracy, and computational efficiency of our method against benchmark approaches. Section 3 extends the application to the more complex Bloom et al. (2018) model to demonstrate scalability to larger state spaces. Section 4 concludes with a discussion of the broader implications of our approach for macroeconomic modeling and potential future research directions.

1.1 Related Literature

This paper contributes to the literature on solution methods for heterogeneous agent models with aggregate uncertainty, with particular focus on heterogeneous firm models.

First, my work builds on global solution methods for heterogeneous agent models with aggregate uncertainty, particularly the Krusell-Smith framework and its extensions. Den Haan (2010) provides a survey of solution methods for the original Krusell and Smith (1998) model, while Terry (2017) offers a comprehensive survey specifically focused on solution methods for heterogeneous firm models such as Khan and Thomas (2008). A significant challenge in heterogeneous firm models is the high computational cost of simulation. As Terry (2017) and Bloom et al. (2018) emphasize, simulation is often crucial for estimation and calibration, making simulation speed improvements essential. Some methods, such as Algan et al. (2008) and Sunakawa (2020), have been developed to update forecasting rules without relying on simulation. In contrast, my approach does not aim to avoid simulation but rather to accelerate it by incorporating the equilibrium price into the policy function. For local solutions, notable contributions include Reiter (2009), Ahn et al. (2018), Boppart et al. (2018), Winberry (2018), and Auclert et al. (2021). For additional global methods beyond Krusell and Smith (1998), see also Den Haan and Rendahl (2010).

Second, my work leverages recent advances in deep learning techniques for solving macroeconomic models. Fernández-Villaverde et al. (2024) provides a comprehensive survey of this growing field. Several notable contributions include Fernández-Villaverde et al. (2020) and Maliar et al. (2021), who approximate value and policy functions with neural networks by jointly training these functions through minimizing a combined loss function based on the Bellman equation error and first-order conditions. Han et al. (2021) take a different approach by training value and policy functions separately using distinct loss functions. Azinovic et al. (2022) use a neural network for the policy function, approximating the policy function that satisfies equilibrium conditions by including equilibrium conditions in the loss function.

The key distinction of my approach is its specific application to heterogeneous firm models where finding equilibrium prices throughout the simulation process poses a significant computational challenge. While existing methods have made important contributions to both global solutions and deep learning applications in macroeconomics, none have effectively addressed the specific computational bottleneck of repeatedly calculating market-clearing equilibrium prices during simulation of heterogeneous firm models with aggregate uncertainty. By training neural networks to learn optimal responses across the state space, my method eliminates the need for costly repetitive optimization within the simulation loop while maintaining the essential structure of established solution techniques.

2 Method

In this section, I will explain my method based on Khan and Thomas (2008). In their setup, firms differ in terms of their idiosyncratic productivity levels and their capital stocks, while being subject to both idiosyncratic and aggregate shocks.

2.1 Model

The production function employed by firms follows a standard Cobb-Douglas form:

$$y = z\epsilon k^{\alpha} N^{\nu}, \tag{1}$$

where y denotes output, z represents aggregate productivity, ϵ captures idiosyncratic firm-level productivity, k stands for capital, and N denotes labor input.

Firms face productivity shocks at both aggregate and individual levels. Specifically, the idiosyncratic productivity evolves according to an AR(1) process:

$$\log(\epsilon') = \rho_{\epsilon} \log(\epsilon) + \eta'_{\epsilon}, \quad \eta'_{\epsilon} \sim N(0, \sigma^2_{\eta_{\epsilon}}), \tag{2}$$

while aggregate productivity evolves similarly:

$$\log(z') = \rho_{z} \log(z) + \eta'_{z}, \quad \eta'_{z} \sim N(0, \sigma^2_{\eta_{z}}). \tag{3}$$

Capital evolves following the conventional law of motion:

$$k' = (1 - \delta)k + i, \tag{4}$$

where δ is the depreciation rate, and i represents investment.

Firms face fixed adjustment costs when altering their capital stock, which are given by a random draw ξ scaled by the equilibrium wage rate w, represented as:

$$\psi(w) = w\xi, \tag{5}$$

where ξ is an independently and identically distributed random variable drawn from distribution G over $[0, \bar{\xi}]$.

On the household side, a representative agent makes consumption, labor supply, and portfolio decisions. The household maximizes its lifetime utility:

$$W(\lambda; z_i, \mu) = \max_{c, n_h, \lambda'} u(c, 1 - n_h) + \beta \sum_{j=1}^{N_z} \pi_{ij} W(\lambda'; z_j, \mu'), \tag{6}$$

$$u(c, 1 - n_h) = \log c + \phi(1 - n_h) \tag{7}$$

subject to a budget constraint involving consumption c, labor supply n_h, and portfolio holdings λ. Here, μ represents the distribution of idiosyncratic shocks and capital, evolving according to $\mu' = \Gamma(z, \mu)$.

The firm's optimization problem involves choosing employment n and investment k^*, given their current states and adjustment costs:

$$\begin{aligned} v^1(\varepsilon, k, \xi; z, \mu) = \max_{n, k^*} \Big[& z\varepsilon F(k, n) - \omega(z, \mu)\, n + (1 - \delta) k \\ & + \max \Big\{ -\xi\, \omega(z, \mu) + R(\varepsilon, k^*; z, \mu'), \\ & R(\varepsilon, (1 - \delta) k; z, \mu') \Big\} \Big] \end{aligned}$$

while

$$R\left(\varepsilon_e, k'; z_i, \mu'\right) \equiv -\gamma k' + \sum_{j=1}^{N_z} \pi_{ij} d_j\left(z_i; \mu\right) \sum_{m=1}^{N_\varepsilon} \pi^{\varepsilon}_{em} v^0\left(\varepsilon_{\mathrm{m}}, k'; z_j, \mu'\right) \tag{8}$$

$$v^0(\varepsilon, k; z, \mu) \equiv \int_0^{\bar{\xi}} v^1(\varepsilon, k, \xi; z, \mu) G(d\xi) \tag{9}$$

Forecasting rule, (10)

$$\mu' = \Gamma_\mu(z, \mu), \quad p = \Gamma_p(z, \mu) \tag{11}$$

Using the aggregate quantities C and N to describe the market-clearing values of household consumption and hours, we can derive the following from the household's first-order condition:

$$\omega(z, \mu) = \frac{D_2 U(C, 1 - N)}{D_1 U(C, 1 - N)}$$

$$d_j(z, \mu) = \frac{\beta D_1 U\left(C'_j, 1 - N'_j\right)}{D_1 U(C, 1 - N)} \tag{12}$$

Defining $p(z, \mu)$ as the price plants use to value current output (relative to the marginal utility of consumption), we have the two conditions:

$$p(z, \mu) = D_1 U(C, 1 - N) \tag{13}$$

$$\omega(z, \mu) = \frac{D_2 U(C, 1 - N)}{p(z, \mu)} \tag{14}$$

Using the definitions for p and w above, and denoting V as the value function measured in units of household marginal utility, the Bellman equation can be rewritten as:

$$
\begin{aligned}
V^1(\varepsilon, k, \xi; z, \mu) = \max_{n \in \mathbf{R}_+} & (z\varepsilon k^\alpha n^\nu - \omega n + (1-\delta)k)p \\
& + \max \left\{ -\xi\omega p + \max_{k^* \in \mathbf{R}_+} R\left(\varepsilon, k^*; z, \mu'\right), R\left(\varepsilon, (1-\delta)k; z, \mu'\right) \right\}
\end{aligned} \tag{15}
$$

$$
R\left(\varepsilon, k'; z, \mu'\right) \equiv -\gamma k' p + \beta \sum_{j=1}^{N_z} \pi_{ij} \sum_{m=1}^{N_\varepsilon} V^0\left(\varepsilon_m, k'; z_j, \mu'\right),
$$

$$
V^0(\varepsilon, k; z, \mu) \equiv \int_0^{\bar{\xi}} V^1(\varepsilon, k, \xi; z, \mu) G(d\xi)
$$

Forecasting rule,

$$
\mu' = \Gamma_\mu(z, \mu), \quad p = \Gamma_p(z, \mu)
$$

Note that the second maximization in (15) reflects the firm's choice between investing to move to the new capital level k^* or remaining at the depreciated level $(1-\delta)k$. Importantly, the choice of k^* depends only on (z, ε, μ) and **not** on the firm's individual capital k.[1]

The threshold level of the adjustment cost ξ that determines whether the firm invests is given by:

$$
\xi^* = \frac{R(\varepsilon, k^*; z, \mu') - R(\varepsilon, (1-\delta)k; z, \mu')}{p\omega} \tag{16}
$$

The Bellman equation we actually solve is the one integrated over the distribution of ξ:

$$
\begin{aligned}
V^0(\varepsilon, k; z, \mu) = \max_{n \in \mathbf{R}_+} \Big[& \big(z\,\varepsilon\,k^\alpha\,n^\nu \;-\; \omega\,n \;+\; (1-\delta)\,k\big)\,p \\
& + \;\alpha(z, \varepsilon, \mu)\Big(-\,\omega\,p \int_0^{\bar{\xi}} \xi\,G(\mathrm{d}\xi) \;+\; \max_{k^* \in \mathbf{R}_+} R\big(\varepsilon, k^*; z, \mu'\big)\Big) \\
& + \;\big(1 - \alpha(z, \varepsilon, \mu)\big)\; R\big(\varepsilon, (1-\delta)\,k; z, \mu'\big)\Big].
\end{aligned} \tag{17}
$$

Here, $\alpha(z, \varepsilon, \mu)$ denotes the probability of adjustment, which is given by $\alpha(z, \varepsilon, \mu) = G(\xi^*) = \xi^*/\bar{\xi}$.

2.2 Krusell-Smith (KS) Method

The most problematic aspect of solving this model is $\mu(\varepsilon, k)$, which is an infinite-dimensional object. This leads to an infinite number of state variable combinations, making the model unsolvable. Therefore, following Krusell and Smith (1998), we approximate $\mu(\varepsilon, k)$ with aggregate capital K. They interpret this as bounded rationality.[2] Consequently, $\mu(\varepsilon, k)$ in equation (17) and forecasting rules is replaced by K, resulting in the following equation:

[1]Since the adjustment cost $\xi\omega p$ is independent of k, the optimal choice of k^* is also independent of it.

[2]Han et al. (2021) construct generalized moments using a neural network, where $\mu(\varepsilon, k)$ is composed of a finite number of agents.

$$\begin{aligned} V^0(\varepsilon, k; z, K) = \max_{n \in \mathbf{R}_+} \Big[& \big(z\, \varepsilon\, k^{\alpha}\, n^{\nu} \;-\; \omega\, n \;+\; (1-\delta)\, k \big)\, p \\ & + \; \alpha(z, \varepsilon, K) \Big(-\omega\, p \int_0^{\bar{\xi}} \xi\, G(\mathrm{d}\xi) \;+\; \max_{k^* \in \mathbf{R}_+} R\big(\varepsilon, k^*; z, K'\big) \Big) \\ & + \; \big(1 - \alpha(z, \varepsilon, K)\big)\; R\big(\varepsilon, (1-\delta)\, k; z, K'\big) \Big] \end{aligned} \tag{18}$$

$$R\left(\varepsilon, k'; z, K'\right) \equiv -\gamma k' p + \beta \sum_{j=1}^{N_z} \pi_{ij} \sum_{m=1}^{N_\varepsilon} V^0\left(\varepsilon_m, k'; z_j, K'\right) \tag{19}$$

$$\log(K') = a_K + b_K \log(K) \tag{20}$$

$$\log(p) = a_p + b_p \log(K) \tag{21}$$

Forecasting rules are assumed to take the log-linear form. Equation (18) has two maximization problems on the right-hand side. The first maximization is with respect to n, which is determined by the first-order condition. The second maximization is with respect to k^*. This involves finding the k^* that maximizes R in equation (19), given the values from the forecasting rules (20) and (21), using a numerical optimization algorithm.

Algorithm 1: Krusell-Smith Method Procedure

```
1  Initialize: Set initial forecasting rule parameters and define the state grid;
2  **repeat**
3      **Step 1: Solve the Bellman Equation**;
4      Given forecasting rules, do value function iteration;
5      **Step 2: Simulate the Model**;
6      Run 2500 periods simulations using the obtained value function;
7      **Step 3: Update Forecasting Rules**;
8      Update parameters by regressing simulation outcomes;
9      **Step 4: Check Convergence**;
10     If$\| \log V' - \log V \| < \epsilon$, then terminate; otherwise, set $n \leftarrow n + 1$;
11 **until** *convergence condition* $\| \log V' - \log V \| < \epsilon$ *is satisfied*;
12 **Output:** Value, policy function and converged forecasting rule parameters;
```

Algorithm 1 shows the solution procedure. In the KS algorithm, we first determine the range and number of grid points for each state variable. Terry (2017) use 5, 5, 10, and 10 grid points for ε, z, k, and K, respectively. Interpolation is performed for k and K. Then, in Step 1, solve the bellman equation. In the typical Value Function Iteration(VFI), the right-hand side of equation (18) is calculated for all combinations of ε, z, k, and K. This value is then used as the new V, and the right-hand side of equation (18) is calculated again. This process continues iteratively until convergence, at which point Step 1 is complete. During this process, K' and p in the equation are determined according to equations (20) and (21).

In Step 2, we perform a simulation using the value function obtained in Step 1. Since the simulation is a crucial aspect of my proposed solution method, let's examine its contents in detail. Algorithm 2 presents a simplified algorithm for the simulation.

Algorithm 2: Simulation with Price Bisection (KS Method)

```
for $t = 1, \dots, 2500$ periods do
    while price has not converged do
        Guess the equilibrium price: $p_{guess}$;
        for each state combination $(\varepsilon, k)$ do
            for each candidate action $(k')$ do
                Compute the right-hand side of the Bellman equation;
            end
            Search for the combination that maximizes the right-hand side;
        end
        Aggregate and compute excess demand;
        Update the price interval based on excess demand;
    end
end
```

While the VFI for the Khan and Thomas (2008) model takes only about 2 seconds, the subsequent simulation requires approximately 3 minutes per iteration, consuming the vast majority of the computational time. This is due to p being implicitly determined, depending on the distribution itself. While Krusell and Smith (1998) could explicitly derive the interest rate from K using the representative firm's first-order condition, in Khan and Thomas (2008), the price depends on the entire distribution. Although the distribution is approximated by a histogram in practice, we calculate optimal actions at each point in this histogram and compute the following value:

$$C(z, \mu) = \int \left[z_i \varepsilon k^\alpha n^\nu - \int_0^{\bar{\xi}} \left(k'(\varepsilon, k, \xi; z, \mu) - (1-\delta)k \right) G(d\xi) \right] \mu(d\varepsilon \times dk) \tag{22}$$

This equation is an equilibrium condition stating that output minus net of investment, is consumed in aggregate. From equation (13) and the household's optimization condition, we have:

$$p(z, \mu) = \frac{1}{C(z, \mu)} \tag{23}$$

Ultimately, the simulation requires that equation (23) holds in each period, and the fixed point p is found using the bisection method in each period. $C(z, \mu)$ includes k', which is either k^* or $(1-\delta)k$. k^* is chosen to maximize (19). Since (19) includes p, the bisection method requires recomputing k^* for each new guess of p. More precisely, the choice of k^* computed during the VFI step is optimal under the perceived law of motion given by the forecasting rules (20) and (21). However, during the simulation's price bisection, we search for the *actual* market-clearing price that satisfies (23). The prices guessed within this bisection search, p_{guess}, may differ from the price implied by the forecasting rule (21) for the current aggregate state K. Thus we need to have re-optimization for every price determined by bisection. This re-optimization step corresponds to the computationally intensive innermost loop depicted in Algorithm 2. For each guess of p, the value of $R(\varepsilon, k^*; z, K')$ is calculated for *all* grid points of k, given ε, z and K', and the k that maximizes it is chosen. This process is performed for every point in the histogram each time p is updated. In the code of Terry (2017), this calculation is done for 5×10 points in the (ε, k) histogram. As can be easily seen, the computational burden increases as the number of state variables and their corresponding grid points that constitute the distribution increase. As we will see in the next chapter, the histogram in Bloom et al. (2018) consists of 16,835 points.

2.3 My Method

As seen in the previous section, the problem with the KS method lies in the need to recompute optimal actions every time the price is updated. Therefore, this issue can be resolved by constructing a policy function that includes the price as a state variable. In my method, both the policy function and the value function are approximated using neural networks and policy function include price as a state variable. Furthermore, to serve as a more general solution method, I also approximate the forecasting rules with neural networks, following Fernández-Villaverde et al. (2023). There are pros and cons to using log-linear regression versus neural networks for the forecasting rules in terms of speed and accuracy. Therefore, I will discuss this in later. In the following, I will describe the version where the forecasting rules are also approximated by neural networks.

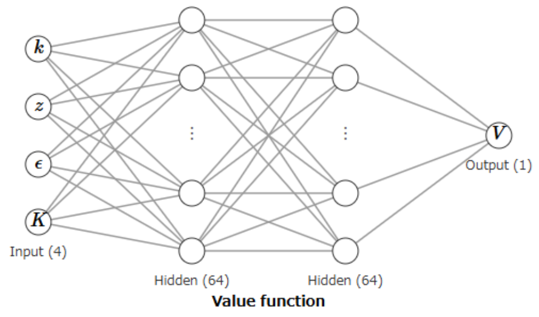

(a) Value Function Approximation

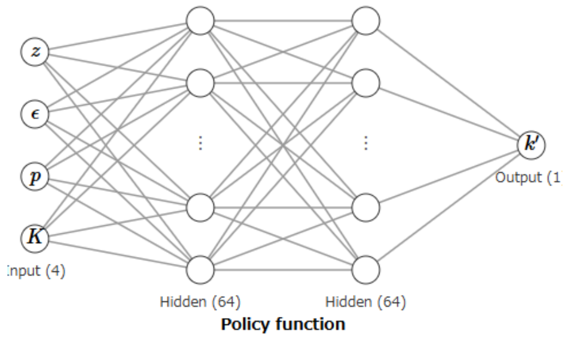

(b) Policy Function Approximation

Figure 1: Neural Network Approximations

Specifically, the value and policy functions in equation (17) are approximated with neural networks as follows:

$$V^0(\varepsilon, k; z, \mu) \approx V^0_{nn}(\varepsilon, k; z, K)\,, \tag{24}$$
$$k^* \approx g_{nn}(z, \varepsilon, p, K)\,. \tag{25}$$

Figures 1a and 1b show snapshots of the value and policy functions, respectively. The neural networks have 2 hidden layers with 64 neurons per layer. The value function takes the state variables directly as input and outputs the value. The policy function's inputs are z, ε, p, and K. As mentioned in Section 2.1, the choice of k^* is a function of z, ε, and K. Therefore, I add the price as a state variable. By including the price, I avoid the need to re-optimize k^* for each price update during the bisection search in the simulation.

Forecasting rules are similarly approximated:

$$\Gamma_\mu(z, \mu) \approx \Gamma^\mu_{nn}(z, K)\,, \tag{26}$$
$$\Gamma_p(z, \mu) \approx \Gamma^{nn}_p(z, K)\,. \tag{27}$$

Since the policy function is a function that outputs the k that maximizes (19), it is trained by minimizing the following loss function:

Policy Function Loss:

$$\mathcal{L}_{policy} = -\frac{1}{N}\sum_{i=1}^{N} R\Big(\varepsilon_i, k_i'; z_i, K_i\Big). \tag{28}$$

Where,

$$k_i' = g_{nn}(z_i, \varepsilon_i, p_{error,i}, K_i) \tag{29}$$

$$\begin{aligned} R(\varepsilon_i, k_i'; z_i, K_i) = & -\gamma\, k_i' p_{error,i} \\ & + \beta \sum_{j=1}^{N_z} \pi_{ij} \sum_{m=1}^{N_\varepsilon} \pi_{im} V_{nn}^0(\varepsilon_m, k_i'; z_j, K_i'). \end{aligned} \tag{30}$$

$$p_{error,i} = \Gamma_p^{nn}(z_i, K_i) + error_i, \quad error_i \in [-0.15, 0.15] \tag{31}$$

$p_{error,i}$ is the forecasting rule for p plus a random value taken from $[-0.15, 0.15]$. The reason for adding this noise is to accommodate the price updates during the bisection search in the simulation as stated in the previous section. The policy is trained by minimizing (29) via gradient descent (which is equivalent to maximizing R). The parameters of these neural networks are optimized using the ADAM optimizer with a learning rate of 0.001.

The loss function for the value function is the squared difference between the left-hand side and the right-hand side of the Bellman equation. In standard VFI, the right-hand side is directly used as the updated value function. However, in the neural network-based solution method, I train the network to minimize the difference between both sides. To stabilize the training of the value function, a target network is used. Details are provided in the Appendix.

Value Function Loss:

$$\mathcal{L}_V = \frac{1}{N}\sum_{i=1}^{N}\Big(V_{nn}^0(\varepsilon_i, k_i; z_i, K_i) - \mathrm{RHS}_i\Big)^2. \tag{32}$$

Where,

$$\begin{aligned} \mathrm{RHS}_i = & \left(z_i \varepsilon_i k_i^\alpha n_i^\nu - \omega_i n_i + (1-\delta)k_i\right) p_i \\ & + \alpha(z_i, \varepsilon_i, K_i)\left[-\omega_i p_i \int_0^{\bar{\xi}} \xi_i G(d\xi_i) + R\left(\varepsilon_i, k_i^*; z_i, K_i'\right)\right] \\ & + (1 - \alpha(z_i, \varepsilon_i, K_i))\, R\left(\varepsilon_i, (1-\delta)k_i; z_i, K_i'\right). \end{aligned} \tag{33}$$

$$R(\varepsilon_i, k_i^*; z_i, K_i') = -\gamma k_i^* p + \beta \sum_{j=1}^{N_z} \pi_{ij} \sum_{m=1}^{N_\varepsilon} V_{nn}^0\left(\varepsilon_m, k_i^*; z_j, K_i'\right) \tag{34}$$

$$k^* = g_{nn}(z_i, \varepsilon_i, p_i, K_i) \tag{35}$$

2.4 Results

In this section, I compare the performance of our proposed method with the benchmark Krusell-Smith (KS) method. For the KS method, I use the Fortran code provided by Terry (2017). Proposed method is implemented in Python using the PyTorch library. The parameter settings and histogram grid specifications are identical across all methods. Computations were performed on a system with a Core(TM) i7-12700F 2.10 GHz CPU and a GeForce RTX 3080 GPU. I focus on several important dimensions: (i) computation time, (ii) the Bellman equation error, (iii) the dynamics of macroeconomic variables in an unconditional simulation, (iv) key microeconomic moments of the investment rate, and (v) the accuracy of the forecast rules. I present results labeled "My method (reg)" when using log-linear regression for the forecasting rule, and "My method (NN)" when using neural networks for the forecasting rule.

Computational Speed Comparison First, I show computation speed. Table 1 compares computation time.

Method	VFI Time (sec)	Simulation Time (sec)	Total Time (min)
KS method (Terry (2017))	3	193	24
My method (reg)	123	68	14
My method (NN)	130	219	37

Table 1: Computation time comparison

The VFI and simulation times reported in the table are measured during the first iteration of the outer loop. For the simulations, the KS method and My method (reg) use a simulation length of 2,500 periods, while My method (NN) uses a longer simulation of 8,000 periods for the stability of forecasting rules. It is worth noting that, from the second iteration onward, the VFI step in My method benefits from using the previous iteration's results as a warm start, significantly reducing the computation time to approximately 30 seconds per iteration. All reported total times are the cumulative results of six iterations of the outer loop.

Bellman Equation Error Table 2 reports the results of a Bellman error comparison, where the error is measured as $\log V' - \log V$ for a set of state points.

Table 2: Bellman equation error: $\log V' - \log V$.

Method	**Bellman Error** ($\log V' - \log V$)
KS method (Terry (2017))	0.0157
My method	0.0086

In the both method, it evaluates the maximum Bellman error across 250 grid points, where the grid is constructed by taking 5 points for the aggregate shock z, 5 for the idiosyncratic shock ε, 10 for individual capital k, and 10 for the aggregate capital K. As shown in Table 2, the NN method achieves a lower Bellman error (0.0086) compared to the KS method (0.0157), indicating that my neural network approximation yields more accurate value functions over the sampled domain.

Unconditional Simulation Comparison Next, I assess how the approximate policies perform in a long-run (unconditional) simulation. Figure 2 compares the time paths for aggregate output and investment between the KS method and our NN method for same realization of shocks.

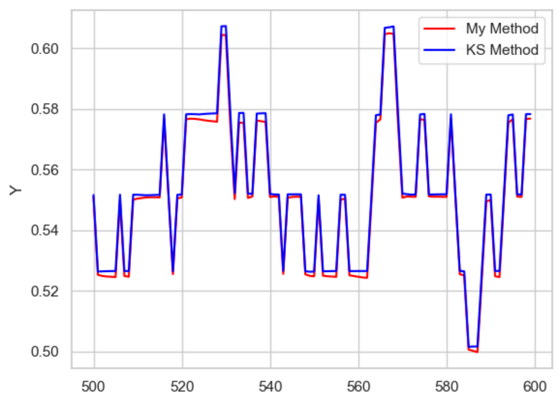

(a) Aggregate output

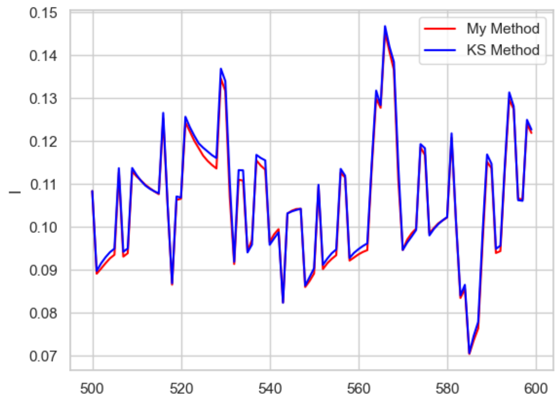

(b) Aggregate investment

Figure 2: Comparison of unconditional simulation paths between KS and NN methods.

The aggregate time paths under my NN method track those from the KS method closely. Despite relying on neural networks for approximating the policy function and value function, the NN method captures the dynamics of aggregate output and investment with high fidelity.

Microeconomic Investment-Rate Moments Table 3 reports key microeconomic investment-rate moments. I present our NN method side-by-side with the KS method.

Table 3: Microeconomic investment-rate moments. For KS, we reproduce the results from Terry (2017).

	KS	**My method (reg)**	**My method (NN)**
$\frac{i}{k}$	0.0947	0.1075	0.1019
$\sigma\left(\frac{i}{k}\right)$	0.2597	0.3524	0.3214
$\mathbb{P}\left(\frac{i}{k}=0\right)$	0.7693	0.7347	0.7414
$\mathbb{P}\left(\frac{i}{k}\geq 0.2\right)$	0.1724	0.1717	0.1714
$\mathbb{P}\left(\frac{i}{k}\leq -0.2\right)$	0.0280	0.0394	0.0331
$\mathbb{P}\left(\frac{i}{k}>0\right)$	0.1890	0.2124	0.2152
$\mathbb{P}\left(\frac{i}{k}<0\right)$	0.0417	0.0528	0.0528

Proposed NN-based method generates micro-level investment statistics that are very close to those produced by the KS method. To verify the difference the value between them, I will do some experiments.

Forecast-System Accuracy Table 4 reports measures for the forecast of the aggregate price p and next-period aggregate capital K', comparing my NN method to KS.
As can be seen from the table, the KS method exhibits the best overall accuracy. My method (reg), which uses log-linear regression for the forecasting rule, achieves comparable or slightly lower

Table 4: Internal accuracy of forecasting rules for the aggregate price p and next-period capital K'. Values for KS are reproduced from Terry (2017).

	p (%)			K' (%)		
	My (reg)	My (NN)	KS	My (reg)	My (NN)	KS
Den Haan Statistics						
Max	0.53	0.75	0.11	0.89	2.08	0.39
Mean	0.07	0.12	0.06	0.16	0.33	0.25
Root Mean Squared Error (RMSE)						
RMSE	0.09	0.14	0.05	0.08	0.14	0.05
Forecast Regression R^2						
R^2	0.9994	0.9983	0.9998	0.9948	0.9995	0.9995

accuracy, but is still quite accurate. On the other hand, the forecasting rule using neural networks (My method (NN)) shows relatively lower accuracy. Two potential reasons can be considered for this. First, the overall error levels are very small. The RMSE for p in Table 4 is presented in percentage terms; however, when measured on the original scale, the RMSE is 0.0008 (and the MSE is 6.4×10^{-7}). Second, the number of training samples for the forecasting rule is limited. The training samples for the forecasting rule are drawn from the preceding simulation. If there are differences in the realizations of shocks, some shocks may not be sufficiently learned. Unlike linear regression, neural networks share parameters across different shock realizations, making them potentially more susceptible to this issue.

Therefore, the choice between using log-linear regression or neural networks for the forecasting rule should depend on the desired speed, accuracy, and the ability to capture nonlinearities. A key advantage of My method is the ease with which these components can be interchanged.

3 Application to the Model of Bloom et al. (2018)

In this section, I demonstrate that the efficiency of my method becomes even more pronounced in larger models. I apply my method to the model of Bloom et al. (2018), which incorporates both aggregate and idiosyncratic stochastic volatility shock for firm productivity, as well as nontrivial capital and labor adjustment costs. Below, I provide a brief overview of the production environment and demonstrate how my neural-network-based solution can handle the large state space more efficiently than traditional methods.

3.1 Model

Each firm j produces output at time t according to

$$y_{j,t} = A_t z_{j,t} k_{j,t}^{\alpha} n_{j,t}^{\nu}, \tag{36}$$

where A_t is an aggregate productivity process, $z_{j,t}$ is idiosyncratic productivity, and $k_{j,t}$ and $n_{j,t}$ are firm-specific capital and labor, respectively. Both A_t and $z_{j,t}$ follow persistent stochastic processes with time-varying volatility (σ^A_{t-1} and σ^Z_{t-1}), capturing switches between "low-uncertainty" and "high-uncertainty" regimes. Capital evolves via

$$k_{j,t+1} = (1-\delta_k)\,k_{j,t} + i_{j,t}, \tag{37}$$

with investment $i_{j,t}$ subject to a fixed adjustment cost and partial irreversibility. Labor $n_{j,t}$ also faces adjustment frictions:

$$n_{j,t} = (1-\delta_n)\,n_{j,t-1} + s_{j,t}, \tag{38}$$

where δ_n is an exogenous destruction rate and $s_{j,t}$ net hiring. Each of these choices incurs a fixed cost whenever the firm adjusts, as well as proportional costs dependent on the magnitude of $i_{j,t}$ or $s_{j,t}$. The model's resulting Bellman equation can be written as

$$\begin{aligned}\tilde{V}(k, n_{-1}, z; A, \sigma^A, \sigma^z, \mu) = \max_{i,n} \Bigg\{ & p(A,\sigma^A,\sigma^z,\mu)\Big[y - w(A,\sigma^A,\sigma^z,\mu)n - i - \mathrm{AC}^k - \mathrm{AC}^n\Big] \\ & + \beta \mathbb{E}\Big[\tilde{V}(k', n, z'; A', \sigma^{A'}, \sigma^{z'}, \mu')\Big]\Bigg\}. \end{aligned} \tag{39}$$

Forecasting rules,

$$\mu' = \Gamma_\mu(A,\sigma^A,\sigma^z,\mu), \quad p = \Gamma_p(A,\sigma^A,\sigma^z,\mu). \tag{40}$$

Because of the multiple shocks and the state variables involved—specifically the endogenous states (k, n_{-1}, z) and the aggregate states $(A, \sigma^A, \sigma^Z, \mu)$ determining expectations—the state space expands quickly. In the original code, the firm's problem is solved by discretizing the state space. The number of grid points for each state variable, corresponding to the order $(k, n_{-1}, z, A, \sigma^A, \sigma^Z, \mu)$, is shown below, resulting in a total grid size of:

$$\underbrace{91}_{\substack{\text{grid points}\\ \text{for } k}} \times \underbrace{37}_{\substack{\text{grid points}\\ \text{for } n_{-1}}} \times \underbrace{5}_{\substack{\text{grid points}\\ \text{for } z}} \times \underbrace{5}_{\substack{\text{grid points}\\ \text{for } A}} \times \underbrace{2}_{\substack{\text{states}\\ \text{for } \sigma^A}} \times \underbrace{2}_{\substack{\text{states}\\ \text{for } \sigma^Z}} \times \underbrace{10}_{\substack{\text{grid points}\\ \text{for } \mu}} = 3{,}367{,}000 \quad \text{points.}$$

Here, σ^A and σ^Z represent the two possible volatility regimes (e.g., high/low).

3.2 Result

Computation and Simulation Speed. Table 5 presents the total solution time, VFI time, and simulation time for each method. As the table shows, my method achieves a significant reduction in computation time compared to the KS method. Simulations were run for 5,000 periods for the KS method and my method (reg), and for 15,000 periods for my method (NN) to ensure stability of the forecasting rules. All reported total times are the cumulative results of 16 iterations of the outer loop. Unlike the results for the Khan and Thomas (2008) model in the previous section, I observe a substantial difference in the Value Function Iteration (VFI) time as well.

Method	**Total Time (min)**	**VFI Time (min)**	**Simulation Time (min)**
KS method	2380	29	133
My Method (reg)	50	3.3	1.7
My Method (NN)	95	3.3	4.5

Table 5: Speed comparison for the Bloom et al. (2018) model. VFI time refers to the time required to solve the bellman equation. Simulation time is measured for 5,000 periods for the first simulation.

Sources of Speed Improvement. The dramatic reduction in simulation time, particularly evident in Table 5, stems from two key features of my method. Firstly, as discussed previously, the use of a policy function $g_{nn}(z, \varepsilon, p, K)$ that includes the equilibrium price p as a state variable eliminates the need for repeated optimization of firm actions within the price bisection loop required in each simulation period. Once trained, the policy network provides an instantaneous mapping from the state (including the guessed price) to the optimal action, bypassing the computationally intensive maximization step inherent in the standard KS simulation.

Secondly, I leverage GPU acceleration for the remaining computations within the simulation. Specifically, finding the equilibrium price in each period involves evaluating the policy function, computing firm-level variables (like output and investment) based on the chosen actions, and then aggregating these across all points in the distribution grid to check the market clearing condition (23). In the Bloom et al. (2018) model, this distribution grid consists of 16,835 points, making efficient computation crucial. While the final aggregation step is inherently sequential, the preceding steps—evaluating the neural network policy function and computing resulting variables for each of the 16,835 grid points—are highly parallelizable. Executing these steps on a GPU allows for substantial speed gains compared to a CPU implementation. This parallelization translates into a significant performance difference: while a CPU implementation of my method might process approximately 2 simulation periods per second, the GPU implementation achieves around 50 periods per second. Consequently, the synergy between the pre-trained, price-conditional policy function and GPU-accelerated parallelization explains the drastic improvement in simulation speed observed in Table 5.

Business-Cycle Properties. I'm not sure if I should write it, and if I do, how I should go about it.

Table 6 reports the HP-filtered standard deviation, ratio to output, and correlation with output for key macroeconomic variables. I compare the results from the KS method, my method using log-linear regression for forecasting (My method (reg)), and my method using neural networks for forecasting (My method (NN)).

	KS Method			My Method (Reg)			My Method (NN)		
	Std	Ratio	Corr	Std	Ratio	Corr	Std	Ratio	Corr
Output	1.832	1.000	1.000	1.532	1.000	1.000	1.586	1.000	1.000
Investment	9.634	5.257	0.925	7.508	4.901	0.854	7.908	4.985	0.877
Consumption	0.910	0.501	0.617	1.033	0.674	0.531	0.968	0.610	0.497
Hours	1.644	0.897	0.821	1.260	0.823	0.721	1.217	0.767	0.784

Table 6: HP-filtered standard deviations, ratios to output, and correlations with output

Internal Accuracy of Forecast Systems. Table 7 presents the internal accuracy of the forecasting rules for the aggregate price p and next-period aggregate capital K'. I report the Den Haan statistics (maximum and mean), the root mean squared error (RMSE), and the R^2 from forecast regressions.

Table 7: Internal accuracy for forecast performance

	p (%)			K' (%)		
	My (reg)	My (NN)	KS	My (reg)	My (NN)	KS
Den Haan Statistics						
Maximum	4.02	3.56	3.67	6.03	6.04	6.87
Mean	0.87	0.84	0.86	1.91	1.72	1.97
Root Mean Squared Error						
RMSE	0.55	0.46	0.47	0.22	0.26	0.42
Forecast Regression R^2						
R^2	0.9682	0.9799	0.9786	0.9958	0.9959	0.9901

Both of my methods achieve high accuracy in forecasting the aggregate price and next-period capital. The Den Haan statistics, RMSE, and R^2 values are comparable to, or better than, those of the KS method. The neural network forecasting rule (My method (NN)) shows particularly strong performance, with slightly better accuracy metrics than the linear regression forecasting rule (My method (reg)) in several cases.

4 Conclusion

This paper addressed the challenge of efficiently solving heterogeneous agent models where the equilibrium price is determined implicitly. We proposed a novel global solution method that approximates the policy and value functions using neural networks, and, crucially, incorporates the equilibrium price as a state variable within the policy function. The resulting algorithm closely resembles the well-known Krusell-Smith method, making it both versatile and easy to implement.

Our main contributions can be summarized as follows:

- We demonstrated a significant reduction in computation time while maintaining solution accuracy in a global solution setting. This was achieved by leveraging the function approximation capabilities of neural networks and, critically, by including the equilibrium price directly in the policy function.
- We proposed a method that, in addition to its performance benefits, is highly versatile and straightforward to implement, due to its close algorithmic similarity to the widely used Krusell-Smith approach.

References

Ahn, S., G. Kaplan, B. Moll, T. Winberry, and C. Wolf (2018). When inequality matters for macro and macro matters for inequality. *NBER macroeconomics annual 32*(1), 1–75.

Algan, Y., O. Allais, and W. J. Den Haan (2008). Solving heterogeneous-agent models with parameterized cross-sectional distributions. *Journal of Economic Dynamics and Control 32*(3), 875–908.

Auclert, A., B. Bardóczy, M. Rognlie, and L. Straub (2021). Using the sequence-space jacobian to solve and estimate heterogeneous-agent models. *Econometrica 89*(5), 2375–2408.

Bloom, N., M. Floetotto, N. Jaimovich, I. Saporta-Eksten, and S. J. Terry (2018). Really uncertain business cycles. *Econometrica 86*(3), 1031–1065.

Boppart, T., P. Krusell, and K. Mitman (2018). Exploiting mit shocks in heterogeneous-agent economies: the impulse response as a numerical derivative. *Journal of Economic Dynamics and Control 89*, 68–92.

Den Haan, W. J. (2010). Comparison of solutions to the incomplete markets model with aggregate uncertainty. *Journal of Economic Dynamics and Control 34*(1), 4–27.

Den Haan, W. J. and P. Rendahl (2010). Solving the incomplete markets model with aggregate uncertainty using explicit aggregation. *Journal of Economic Dynamics and Control 34*(1), 69–78.

Fernández-Villaverde, J., S. Hurtado, and G. Nuno (2023). Financial frictions and the wealth distribution. *Econometrica 91*(3), 869–901.

Han, J., Y. Yang, et al. (2021). Deepham: A global solution method for heterogeneous agent models with aggregate shocks. *arXiv preprint arXiv:2112.14377*.

Khan, A. and J. K. Thomas (2008). Idiosyncratic shocks and the role of nonconvexities in plant and aggregate investment dynamics. *Econometrica 76*(2), 395–436.

Krusell, P. and A. A. Smith, Jr (1998). Income and wealth heterogeneity in the macroeconomy. *Journal of political Economy 106*(5), 867–896.

Reiter, M. (2009). Solving heterogeneous-agent models by projection and perturbation. *Journal of Economic Dynamics and Control 33*(3), 649–665.

Sunakawa, T. (2020). Applying the explicit aggregation algorithm to heterogeneous macro models. *Computational Economics 55*(3), 845–874.

Terry, S. J. (2017). Alternative methods for solving heterogeneous firm models. *Journal of Money, Credit and Banking 49*(6), 1081–1111.

Winberry, T. (2018). A method for solving and estimating heterogeneous agent macro models. *Quantitative Economics 9*(3), 1123–1151.

A Detailed Forecast Accuracy Statistics: Khan-Thomas Model

This section provides detailed internal accuracy statistics for the forecasting rules used in the Khan-Thomas model application, broken down by aggregate productivity state (A_t). Table 8 compares the benchmark KS method with the log-linear regression (My method (reg)) and neural network (My method (NN)) versions of my proposed method.

Table 8: Internal Accuracy of Forecasting Rules (Khan-Thomas Model)

	Price p			Capital K'		
Statistic	KS	My(reg)	My(NN)	KS	My(reg)	My(NN)
Den Haan Statistics (%)						
Maximum	0.11	0.57	0.76	0.38	1.00	2.08
Mean	0.05	0.09	0.12	0.23	0.23	0.34
Root Mean Squared Error (RMSE) (%)						
$A = A_1$	0.06	0.15	0.08	0.06	0.14	0.08
$A = A_2$	0.05	0.11	0.10	0.05	0.11	0.11
$A = A_3$	0.05	0.04	0.16	0.05	0.06	0.09
$A = A_4$	0.04	0.08	0.11	0.05	0.12	0.08
$A = A_5$	0.04	0.03	0.23	0.05	0.04	0.25
Forecast Regression R^2						
$A = A_1$	1.0000	0.9898	0.9973	1.0000	0.9983	0.9992
$A = A_2$	1.0000	0.9943	0.9968	1.0000	0.9990	0.9990
$A = A_3$	1.0000	0.9992	0.9901	1.0000	0.9996	0.9994
$A = A_4$	1.0000	0.9970	0.9953	1.0000	0.9984	0.9994
$A = A_5$	1.0000	0.9996	0.9749	1.0000	0.9999	0.9933

Notes: Compares internal accuracy statistics for different forecasting methods in the Khan-Thomas model. Den Haan statistics and RMSE are reported as percentage points of log deviation (original values multiplied by 100). R^2 is the standard coefficient of determination. Statistics by Aggregate Shock Level (A_t) correspond to subsamples for each discrete aggregate productivity state. KS Den Haan (Max/Mean) and R^2/RMSE by shock values are from the benchmark source (**?**). **Note: Values reported under RMSE for KS were originally reported as Den Haan statistics by shock in the source.** My(reg) and My(NN) values are calculated from the simulation results of this study.

B Detailed Forecast Accuracy Statistics: Bloom et al. Model

This section provides detailed internal accuracy statistics for the approximate equilibrium forecast mappings used in the Bloom et al. (2018) model application, broken down by the aggregate state (A, S, S_{-1}), representing discretized grid points for aggregate productivity, current uncertainty, and lagged uncertainty. Table 9 compares the benchmark Krusell-Smith (KS) method with my proposed methods using log-linear regression forecasting (My method (reg)) and neural network forecasting (My method (NN)). RMSE values are multiplied by 100.

Table 9: Internal Accuracy Statistics for Forecast Mappings by State (% RMSE) - Bloom et al. Model

Aggregate State	Capital $\log(K_{t+1})$						Price $\log(p_t)$					
(A, S, S_{-1})	KS		My(reg)		My(NN)		KS		My(reg)		My(NN)	
	RMSE	R^2	RMSE	R^2	RMSE	R^2	RMSE	R^2	RMSE	R^2	RMSE	R^2
(1,0,0)	0.43	0.96	0.29	0.99	0.24	0.99	0.60	0.72	0.76	0.75	0.65	0.83
(1,0,1)	0.32	0.98	0.04	1.00	0.70	0.95	0.35	0.91	0.22	0.96	0.33	0.94
(1,1,0)	0.59	0.93	0.45	0.97	0.66	0.98	0.18	0.96	0.19	0.98	0.31	0.97
(1,1,1)	0.49	0.96	0.07	1.00	0.21	1.00	0.26	0.95	0.21	0.97	0.31	0.97
(2,0,0)	0.40	0.98	0.30	0.99	0.25	0.99	0.61	0.84	0.71	0.75	0.55	0.90
(2,0,1)	0.54	0.97	0.07	1.00	0.80	0.94	0.39	0.95	0.20	0.97	0.51	0.88
(2,1,0)	0.32	0.98	0.22	0.97	0.60	0.96	0.28	0.93	0.44	0.66	0.27	0.97
(2,1,1)	0.47	0.98	0.08	1.00	0.24	1.00	0.29	0.96	0.24	0.97	0.34	0.96
(3,0,0)	0.33	0.98	0.24	0.99	0.23	0.99	0.52	0.87	0.63	0.76	0.46	0.91
(3,0,1)	0.35	0.99	0.06	1.00	0.70	0.95	0.40	0.96	0.17	0.98	0.22	0.98
(3,1,0)	0.57	0.95	0.36	0.98	0.43	0.98	0.27	0.95	0.22	0.98	0.53	0.89
(3,1,1)	0.47	0.98	0.08	1.00	0.21	1.00	0.28	0.97	0.25	0.96	0.36	0.95
(4,0,0)	0.39	0.98	0.29	0.99	0.22	0.99	0.58	0.84	0.74	0.70	0.49	0.86
(4,0,1)	0.43	0.98	0.09	1.00	0.73	0.93	0.41	0.90	0.15	0.98	0.16	0.99
(4,1,0)	0.60	0.94	0.33	0.99	0.36	0.99	0.26	0.95	0.22	0.98	0.86	0.78
(4,1,1)	0.47	0.98	0.10	1.00	0.25	0.99	0.28	0.97	0.28	0.93	0.34	0.95
(5,0,0)	0.43	0.97	0.28	0.99	0.25	0.99	0.63	0.77	0.69	0.70	0.44	0.90
(5,0,1)	0.34	0.98	0.13	1.00	0.67	0.89	0.42	0.86	0.14	0.98	0.15	0.98
(5,1,0)	0.27	0.97	0.09	1.00	0.35	0.99	0.26	0.89	0.19	0.98	0.49	0.95
(5,1,1)	0.50	0.97	0.11	1.00	0.22	0.99	0.27	0.96	0.28	0.93	0.33	0.93

Notes: The table shows accuracy statistics for the approximate equilibrium forecast mappings conditional on the aggregate state (A_t, S_t, S_{t-1}) for the Bloom et al. (2018) model. The functional forms are log-linear for KS and My method (reg), and neural networks for My method (NN). Statistics are computed from an unconditional simulation (5000 quarters for KS/reg, 15000 for NN, after discarding initial burn-in). KS values are based on the original benchmark results (*specify source, e.g., Bloom et al. (2018) or supplementary material*). My method (reg) and My method (NN) values are from this study. RMSE represents the root mean squared error of the rule's forecasts within the subsample, multiplied by 100. R^2 is the standard R-squared measure from the relevant forecast regression (or equivalent fit measure for NN) on the subsample.